Anomalous mode in the Raman and ir spectra of mercury telluride

M. L. Bansal,* Alka Ingale,* and A. P. Roy
Solid State Physics Division, Bhabha Atomic Research Centre, Bombay 400 085, India
(Received 7 May 1990)

We discuss the origin of the low-frequency mode occurring at ~ 108 cm^{-1} (at 77 K) in HgTe and Hg-rich $Hg_{1-x}Cd_xTe$. Through temperature- and wavelength-dependent Raman spectra and their analysis, we show that this feature is a combination phonon and acquires significant Raman (ir) activity as a consequence of a Fermi resonance with the TO phonon. Within this framework we are able to explain its TO-phonon-like behavior, and the variation of its frequency, width, and intensity with temperature.

I. INTRODUCTION

Mercury telluride and cadmium telluride are members of the alloy system $Hg_{1-x}Cd_xTe$, an important material for ir applications.[1] The special interest in HgTe and Hg-rich $Hg_{1-x}Cd_xTe$ arises because they provide a unique system where lattice vibrations and electronic excitations (interband and intraband) overlap in energy. Both the end members HgTe and CdTe and, to a certain extent, their alloys have been investigated using ir reflectivity,[2,3] Raman scattering,[4,5] and neutron scattering[6] to understand their vibrational properties.

In the ir spectra of HgTe (Ref. 2) and $Hg_{1-x}Cd_xTe$ ($x<0.3$),[3] apart from the usual allowed TO phonon at 117 cm^{-1}, an additional mode has been observed below this frequency. Its oscillator strength increases and its frequency decreases with increasing temperature.[2] Raman measurements[4,5] that have been carried out on HgTe at liquid-nitrogen temperature also reveal the presence of an additional feature at ~ 108 cm^{-1}, apart from the usual TO- and LO-phonon modes at 117 and 137 cm^{-1}, respectively. No detailed temperature-dependent Raman study has been reported in literature on HgTe. Swiatek *et al.*[7] observed a similar structure in *p*-type HgTe. Grynberg *et al.*,[2] on the basis of temperature-dependent ir work, found that this additional feature, which they call Ω_2 (we will follow the same notation), has TO-phonon character. Though no definitive assignment of this Ω_2 mode has been made in Ref. 2, several possibilities are discussed. These include absorption due to combination phonon, an impurity-activated zone-edge phonon, a gap mode due to Hg substituting for Te, etc. Witowski and Grynberg[8] observed a similar feature in HgSe. They have argued[8,9] that in these materials $\Gamma_8^V \rightarrow \Gamma_8^C$ electronic interband transitions overlap with the phonon in energy, which can lead to resonant enhancement of the two-phonon cross section. Another school of thought[10] believes this mode to be a gap mode arising as a consequence of Hg substituting for Te in HgTe.

We show in this paper that none of the mechanisms stated above provides a satisfactory explanation of the occurrence of the Ω_2 mode. With a view to understanding its origin, we have carried out temperature- and wavelength-dependent Raman measurements on HgTe. The experimental details and our main results are presented in Sec. II. We demonstrate by a careful analysis of the Raman data that the additional feature Ω_2 can be understood in the framework of a mode coupling between the TO phonon and a difference phonon $[\omega_{TO}(\mathbf{q})-\omega_{TA}(\mathbf{q})]$. In Sec. III, after briefly presenting results of the mode-coupling theory, we apply it to the present case of HgTe and calculate the Raman line shapes. Section IV is devoted to a discussion and comparison of our model with earlier work. Finally we summarize our main conclusions in Sec. V.

II. EXPERIMENTAL RESULTS

In order to rule out the effect of surface and sample quality on the intensity or frequency of the Ω_2 mode, we have carried out investigations on the following three samples of (111)-oriented HgTe.

(a) HgTe obtained from the Solid State Physics Laboratory, New Delhi. The optical-quality surface was produced with mechanical and chemomechanical (0.1 vol.% Br_2–methanol solution) polish. This was finally free etched in 0.01 vol.% Br_2–methanol solution and washed in methanol.

(b) HgTe obtained from Purdue University. The sample was polished with 0.25-μm diamond powder and cleaned in ether and methanol to generate a rough surface.

(c) HgTe same as sample (b) but with an optical-quality surface, produced with the same method as used for sample (a).

The Raman setup used for measurements is described in Ref. 5. The temperature was varied using a two-stage cryogenic refrigerator supplied by Air Products. Two lines at 4965 Å (Ar^+ laser) and 5309 Å (Kr^+ laser) with power ~ 100 mW were used to record the spectra at various temperatures. This choice of wavelengths was made with a view to ascertain whether the scattering mechanisms for the two modes (Ω_2 and the TO phonon) are the same or different ones. 5309 Å is very near the E_1 peak,

whereas 4965 Å is in the flat region of the resonance curve (see Fig. 4 of Ref. 5). The Raman spectra obtained from the (111) face of HgTe [sample (c)] using the 4965-Å excitation are shown in Fig. 1 at various temperatures. Similar spectra were obtained on other samples and at 5309 Å (see Fig. 6). Since for both exciting wavelengths the spectra are identical, henceforth we will present results only for $\lambda = 5309$ Å.

In Fig. 2, we show the variation of frequency difference $(\omega_{TO} - \Omega_2)$ as a function of the temperature for the three samples. We have plotted the difference instead of actual

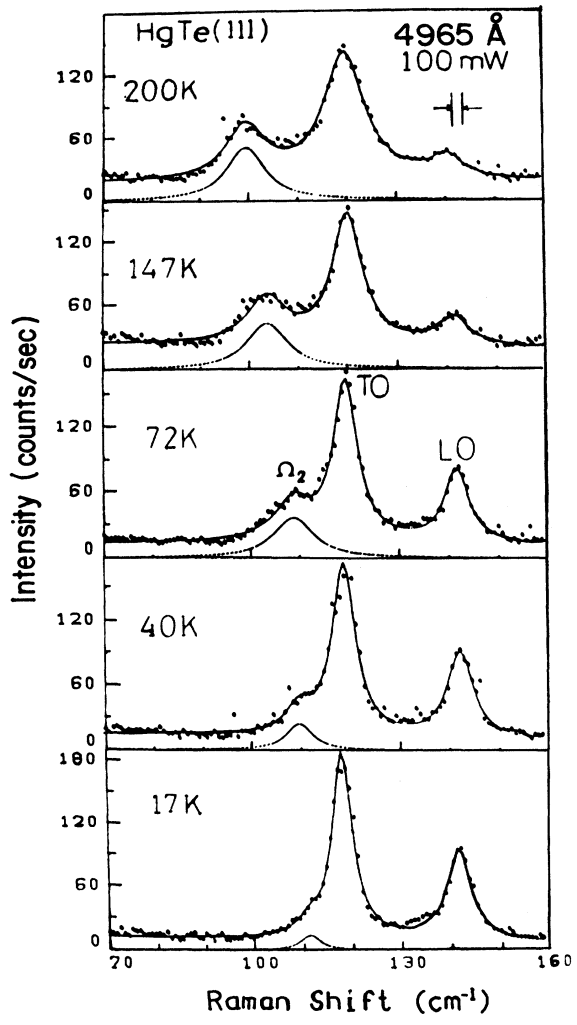

FIG. 1. Raman spectra in backscattering geometry from the (111) face of HgTe. The spectra were recorded with about 100 mW of laser power at 4965 Å. The solid curve represents the least-squares fit using three Lorentzians and the background. The strong feature at ~ 118 cm^{-1} is the TO-phonon mode with a shoulder (or side peak). This side peak is the *additional feature,* which we have labeled Ω_2. The dashed curve represents the Lorentzian used for the Ω_2 mode and brings out its frequency and intensity variation with temperature. The highest-frequency feature at around 140 cm^{-1} is the LO-phonon mode and is not relevant here.

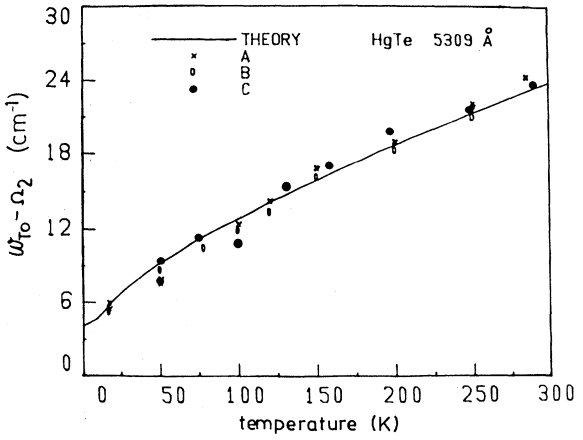

FIG. 2. The figure shows the difference between the frequencies represented by the two peaks labeled Ω_2 and TO (see Fig. 1) as a function of temperature. The solid curve is calculated using the mode-coupling theory.

frequencies to avoid the run-to-run variation of absolute values of frequencies. Variation of Γ_{TO} [full width at half maximum (FWHM)] with temperature for the TO phonon is shown in Fig. 3. The solid curves in these figures are obtained from theory (see Sec. III). Summarizing the various observations, we note the following. (i) Samples (a), (b), and (c) display similar spectra in terms of frequency and intensity of the Ω_2 mode relative to that of the TO-phonon mode. The width of the Ω_2 mode is also sample independent. (ii) The intensity ratio $I(\Omega_2)/I(\mathrm{TO})$ at the two different excitation wavelengths 5309 and 4965 Å are the same and dependent on the temperature alone. This implies that the electronic bands involved in the scattering process are the same ones for both modes. A

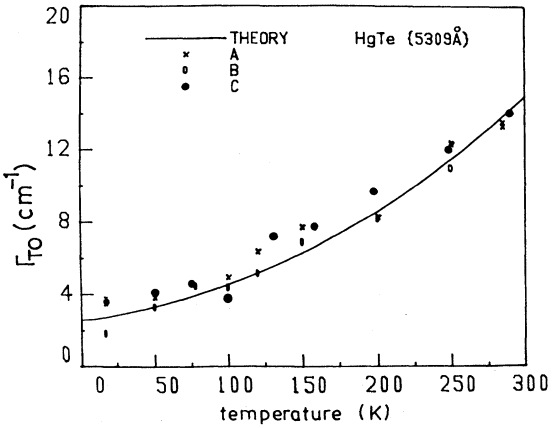

FIG. 3. Full width at half maximum of the TO phonon as a function of temperature. The solid line has been calculated using the expression $\Gamma_{TO} = 2.6 + 0.545\{n(\omega_{TA}(q))[n(\omega_{TO}(q))+1]\}$ cm^{-1}. This assumes that the entire width is due to the decay of the TO phonon into simultaneously creating and annihilating phonons TO($\mathbf{q}$) and TA($\mathbf{q}$), respectively.

similar conclusion has been drawn using all the available lines of Ar^+ and Kr^+ lasers for a fixed temperature (90 K) in Ref. 11. (iii) The intensity ratio $I(\Omega_2)/I(\mathrm{TO})$ is the same for scattering from the two faces (111) and (110). This implies that the Raman tensors for the two modes have the same symmetry. (iv) The frequency of the TO-phonon mode shows an increase of about 2 to 3 cm^{-1} in going from 10 to 290 K, whereas the frequency of the Ω_2 feature decreases from 112 cm^{-1} (20 K) to about 95 cm^{-1} (290 K).

Thus we see that the Ω_2 feature is intrinsic to HgTe and does not depend upon surface condition or sample quality. Observations (ii) and (iii) above imply that symmetry of the Raman tensor for the two modes (Ω_2 and ω_{TO}) is the same; further, the modes have similar scattering mechanism. Finally we have a slight hardening of the TO phonon (contrary to normal softening) with increasing temperature observed in the present work as well as earlier ir experiments.[2] All these observations are logical consequences if we assume that we have here a case of interacting or coupled modes with interaction increasing with the temperature and pushing the modes (Ω_2 and TO) away from each other. With this aim in view, we recapitulate coupled-mode theory and apply it to the present case of HgTe in the following section.

III. THEORY

Raman (Stokes) scattering intensity $S(\omega)$ for modes of transverse type can be related to the imaginary part of the susceptibility $\chi''(\omega)$ by means of the fluctuation-dissipation theorem[12]

$$S(\omega)=R\chi''(\omega)[n(\omega)+1]\ , \tag{1}$$

where $n(\omega)=(e^{\hbar\omega/k_BT}-1)^{-1}$ and R is a constant depending upon the scattering mechanism. $\chi(\omega)$ for the coupled modes in terms of the Green's function $G_{ij}(\omega)$ and the mode strengths P_i and P_j can be written as[12,13]

$$\chi(\omega)=\mathrm{Im}\sum P_iP_jG_{ij}(\omega)\ . \tag{2}$$

The expression for $G_{ij}(\omega)$ is determined by means of the coupled-mode equation

$$\begin{bmatrix}\omega_1^2-\omega^2+i\omega\Gamma_1 & \Delta^2+i\omega\Gamma_{12}\\ \Delta^2+i\omega\Gamma_{12} & \omega_2^2-\omega^2+i\omega\Gamma_2\end{bmatrix}\begin{bmatrix}G_{11} & G_{12}\\ G_{21} & G_{22}\end{bmatrix}=\begin{bmatrix}1 & 0\\ 0 & 1\end{bmatrix}. \tag{3}$$

As described by Barker and Hopfield,[14] there is an infinite variety of choices for the diagonalization of $[G(\omega)]^{-1}$ in Eq. (3). Since $G(\omega)$ is complex, we may arbitrarily diagonalize either the real ($\Delta=0$) or the imaginary ($\Gamma_{12}=0$) part independently. The choice is essentially equivalent to the choice of phases for the interacting modes.[13]

Thus, in principle, it is possible to calculate the Raman line shape for a system of two coupled modes in terms of the seven parameters ω_1, ω_2, Γ_1, Γ_2, Δ, Γ_{12}, and the ratio P_1/P_2. These seven parameters are not really arbitrary. Using a range of measurements (temperature, pressure, etc.) it should be possible to correlate these with measured properties and associate a physical significance with these. A detailed discussion of this point is beyond the scope of this paper and the interested reader is referred to the two articles by Scott.[12,15]

The coupling between two excitations in a molecule, one of which is a one-quantum level and the other of which is a two-quantum state, is known as a *Fermi resonance*. The idea that a Fermi resonance would exist between phonons in ionic crystals was first put forth by Scott.[16] Basically, in a Fermi resonance the allowed TO phonon has finite oscillator strength whereas the overtone can be assumed to have zero oscillator strength. The observed strength of the overtonelike mode is a consequence of wave-function mixing.

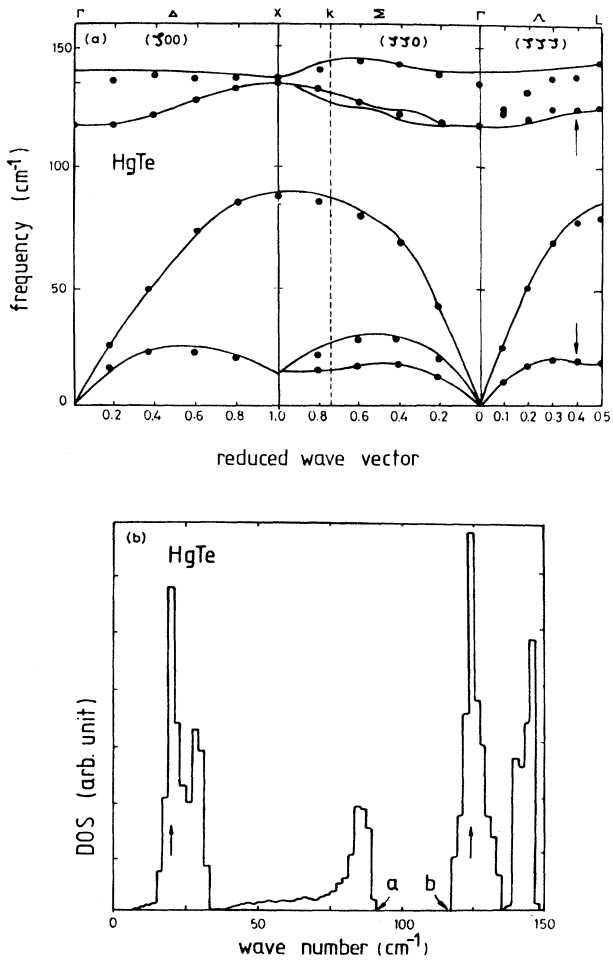

FIG. 4. (a) Phonon-dispersion curves in HgTe at room temperature. The two branches leading to a large density of states at $\omega_{\mathrm{TO}}(q)-\omega_{\mathrm{TA}}(q)$ ($=\Omega_D$) of interest are indicated by arrows (this figure was reproduced from Ref. 10, with permission of the authors and publishers). (b) One-phonon density of states for HgTe. Notice the high density of states at frequencies of interest (this figure was reproduced from Ref. 10, with permission of the authors and publishers).

In HgTe an examination of dispersion curves and the density of states reveals that no overtone is close in frequency to the $\mathbf{q}=\mathbf{0}$ TO phonon. However, as seen in Fig. 4(a),[6,10] the difference phonon $\omega_{\mathrm{TO}}(\mathbf{q})-\omega_{\mathrm{TA}}(\mathbf{q})$ with $\mathbf{q}$ along (111) is close in frequency to the zone-center TO phonon and will have the same symmetry as the TO phonon. Moreover, the density of states [Fig. 4(b) (Ref. 10)] also peaks at these TO($\mathbf{q}$) and TA($\mathbf{q}$) frequencies, which will imply a high density of states for the difference frequency $\Omega_D=\omega_{\mathrm{TO}}(\mathbf{q})-\omega_{\mathrm{TA}}(\mathbf{q})$. It may be noted here that the value of 101 cm^{-1} for Ω_D at 300 K (Table I) is in excellent agreement with the difference in the frequencies of the density-of-states peaks [Fig. 4(b)]. The oscillator strength for such a difference phonon may be set equal to zero, since the two-phonon cross section is generally smaller than the one-phonon cross section by three orders of magnitude.

This leads to a significant reduction in the number of independent parameters required for calculating the Raman line shape through the use of Eq. (1). Since one is not interested in calculating the absolute cross section and only one oscillator has finite oscillator strength (TO phonon at $\mathbf{q}=\mathbf{0}$), $R=1$, $P_1=1$, and $P_2=0$. The various parameters and their temperature variation are listed in Table I.

From Table I we see that $\Omega_{\mathrm{TO}}(T)$, $\Gamma_{\mathrm{TO}}(T)$, and $\Gamma_D(T)$ require no further discussions or justification. $\Omega_D(T)$, as would be noticed, has been assumed to have a large thermal anharmonicity of 4 $\mathrm{cm}^{-1}/(100\ \mathrm{K})$. We have arbitrarily associated all the softening with the upper phonon branch $\omega_{\mathrm{TO}}(\mathbf{q})$. However, it is possible that it is actually a partial hardening of the lower branch[17] coupled with a partial softening of the upper branch. This, however, cannot be distinguished in the present model.

Instead of adopting an arbitrary temperature dependence that would be consistent with experimental data, we correlate Δ^2 with the interaction strength W_{12}. Notice that the coupled-mode frequencies $\omega_{\pm}$ are given (for small dampings) by singularities of the G matrix [Eq. (3)], i.e., they are solutions of

$$\begin{vmatrix} \omega_1^2-\omega^2 & \Delta^2 \\ \Delta^2 & \omega_2^2-\omega^2 \end{vmatrix}=0\ , \tag{4}$$

thus

$$\omega_{\pm}^2=(\omega_1^2+\omega_2^2)/2\pm\{[(\omega_1^2-\omega_2^2)^2+4\Delta^4]^{1/2}\}/2\ . \tag{5}$$

For $\omega_1\sim\omega_2$ and small Δ^2, Eq. (4) reduces to

$$2(\omega_1\omega_2)^{1/2}\begin{vmatrix} \omega_1-\omega & \Delta^2/2(\omega_1\omega_2)^{1/2} \\ \Delta^2/2(\omega_1\omega_2)^{1/2} & \omega_2-\omega \end{vmatrix}=0\ . \tag{4'}$$

The eigenvalue equation is[16]

$$\begin{vmatrix} \omega_1-\omega & W_{12} \\ W_{12} & \omega_2-\omega \end{vmatrix}=0\ . \tag{6}$$

Comparing Eqs. (4') and (6) we obtain

$$\Delta^2=2W_{12}(\omega_1\omega_2)^{1/2}\ . \tag{7}$$

TABLE I. Parameters used for the calculation of coupled modes and the Raman line shape in HgTe.

$\omega_1\equiv\Omega_{\mathrm{TO}}(T)=[117.0-0.005T(\mathrm{K})]\ \mathrm{cm}^{-1}$: $\mathbf{q}=\mathbf{0}$, TO-phonon-mode frequency

$\omega_2\equiv\Omega_D(T)=\omega_{\mathrm{TO}}(\mathbf{q},T)-\omega_{\mathrm{TA}}(\mathbf{q},T)$: Difference phonon frequency
$\omega_{\mathrm{TO}}(\mathbf{q},T)=[133.0-0.04T(\mathrm{K})]\ \mathrm{cm}^{-1}$
$\omega_{\mathrm{TA}}(\mathbf{q},T)=20.0\ \mathrm{cm}^{-1}$

Γ_1: Damping parameter for ω_1, the higher-frequency mode. As a first approximation it is set equal to the experimentally observed FWHM $\Gamma_{\mathrm{TO}}(T)$ of the TO-phonon-like higher-frequency mode.

$\Gamma_2\equiv\Gamma_D(T)$: Damping parameter for ω_2. It is used as a parameter to match the line shape. Its value varies from 5 cm^{-1} (20 K) to 10 cm^{-1} (300 K).

$\alpha=26\ \mathrm{cm}^{-1}$
$\Gamma_{12}=0\ \mathrm{cm}^{-1}$
$P_1=1$
$P_2=0$
$R=1$

The resulting coupled modes are labeled as
$\omega_+\equiv\omega_{\mathrm{TO}}$
$\omega_-\equiv\Omega_2$

Following Scott,[12,15] W_{12} can be related to Γ_1 (corresponding to the stronger of the two oscillators) and the frequency difference $(\omega_1-\omega_2)$ at a given temperature

$$W_{12}=\alpha\Gamma_1(T)[\omega_1(0)-\omega_2(0)]/[\omega_1(T)-\omega_2(T)]\ , \qquad (8)$$

where α is a proportionality constant independent of the temperature. The constant α has been obtained using Eq. (5) for ω_+ and ω_- and compared with the frequency difference as shown in Fig. 2.

The variation of unperturbed frequencies Ω_{TO}, Ω_D and the calculated $\omega_+(\omega_{TO})$ and $\omega_-(\Omega_2)$ frequencies [using Eq. (5) and the parameters of Table I] are shown in Fig. 5. It may be noticed that above about 125 K the parameter Δ^2 is essentially temperature independent, leading to almost temperature-independent shifts for the interacting oscillator frequencies Ω_{TO} and Ω_D.

It is straightforward to obtain the Raman line shape for the two modes Ω_2 and ω_{TO} (TO phonon) using Table I and Eq. (1). We should point out here that, strictly speaking, both ω_- and ω_+ are suitable admixtures of the TO phonon and the difference phonon. However, considering the dominant intensity of ω_+ and its presence at 20 K makes the distinction between the TO and Ω_2 phonons a reasonable and useful one. The computed spectral line shapes at three different temperatures are compared with the experimental spectra in Fig. 6. Reasonable agreement is obtained at all the temperatures, considering that the instrumental resolution [half width at half maximum (HWHM) ~ 1.2 cm^{-1}] has not been taken into consideration in the calculation spectra.

It may be mentioned here that the parameters ω_1, ω_2, and α are strongly interrelated. If the fitting is restricted to mode frequencies alone [Eq. (5)], then the choice of the parameters is not unique. However, the values given in Table I are obtained by a simultaneous fitting to mode frequencies as well as mode intensities [Eqs. (1) and (2)]. It may be emphasized here that this leads to a unique choice for the parameters. It is interesting to note from Table I that our analysis suggests a relatively strong temperature dependence [4 cm^{-1}/(100 K)] for the Ω_D mode.

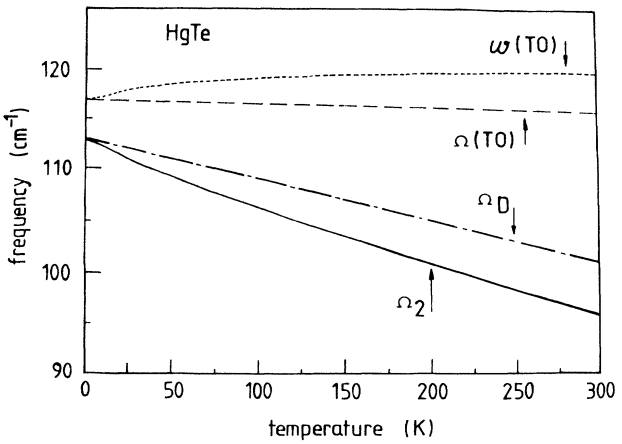

FIG. 5. The figure shows the frequencies of the two interacting oscillators. Uncoupled modes, namely the TO phonon [Ω(TO)] and combination phonon (Ω_D), are assumed to vary linearly with temperature, as shown in Table I. The resulting frequencies for the coupled modes are shown as ω(TO) and Ω_2 in the figure.

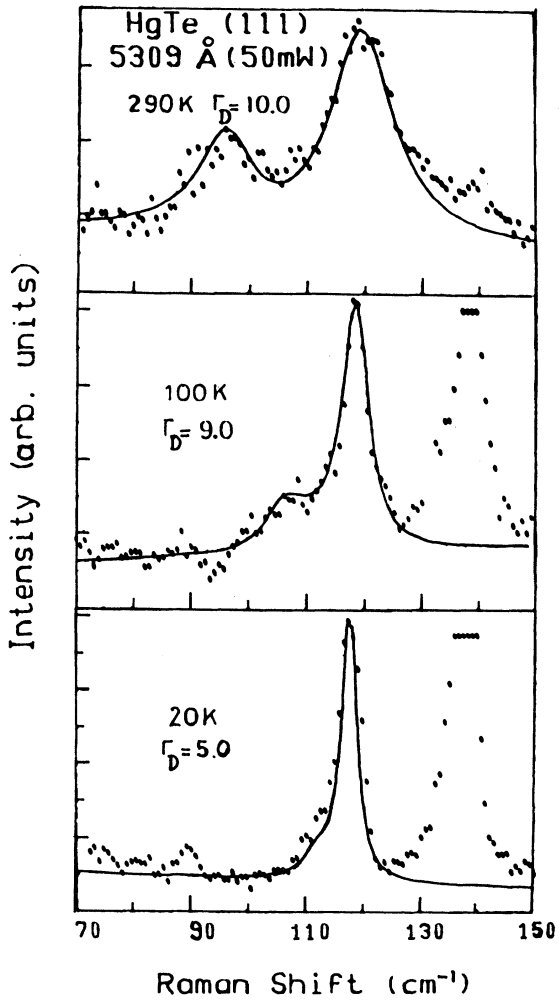

FIG. 6. The solid line is the calculated line shape using Eq. (1). A suitable baseline has been added to each theoretical curve to match the experimentally observed background. The points are experimental spectra. The large intensity at around 140 cm^{-1} is due to the forbidden LO-phonon mode (Ref. 5) and is neither relevant nor included in the present calculation of coupled modes. The slight intensity seen around 89 cm^{-1} is due to the laser plasma line.

IV. DISCUSSION

As we have shown above, the Fermi resonance is able to explain the detailed Raman measurements in HgTe. We discuss here some of the other models that have been proposed in the literature and their inadequacy in explaining the experimental observations.

Defect-activated zone-boundary (DAZB) phonon scattering being the origin of the Ω_2 mode was proposed by Grynberg *et al.*[2] At the time of that analysis phonon-dispersion curves for HgTe were not available. Calculated phonon-dispersion curves[6,10] show a gap in the one-phonon density of states between 92 and 115 cm^{-1}. Thus the DAZB phonon is unlikely to be the origin of the Ω_2 mode. Notwithstanding this, such a process involving the creation of only one phonon, close in frequency to the TO phonon, should lead to a temperature-independent value for $I(\Omega_2)/I(\mathrm{TO})$, contrary to experimental observation.

The gap-mode hypothesis advanced by Talwar and Vandevyver[10] assigns the Ω_2 feature to a gap mode arising as a consequence of Hg substituting for Te in otherwise perfect HgTe. These authors,[10] using a Green's-function formalism, have obtained the correct range of frequency variation exhibited by the Ω_2 mode. In order to understand its large intensity and TO-phonon-like nature, an unacceptably large number of defects have to be invoked. This assumption would suggest sample-specific spectra, which is clearly not the case. This mode occurs in both *n*-type[2] and *p*-type[7] HgTe, with a similar intensity. In addition, this model cannot explain the strong variation of intensity for this mode in ir spectra[2] and Raman spectra (Figs. 1 and 6) as a function of temperature.

We next come to the "two-phonon resonance enhancement" as being the cause of anomalous feature Ω_2.[8,9] As already mentioned, this feature is observed in HgTe,[2,4,7] HgSe,[8] and in Hg-rich $Hg_{1-x}Cd_xTe$.[3] Based on these observations, Witowski and Grynberg[8] suggested that the origin of this feature is a combination phonon with strong oscillator strength arising as a consequence of electronic interband transitions (near the zone center) $\Gamma_8^V \rightarrow \Gamma_8^C$ overlapping in energy with the combination phonon. Surprisingly, such a contribution is not considered for the resonant enhancement of the TO phonon. We show below that an explicit simultaneous consideration of the electronic interband resonant process for both one-phonon and combination phonons leads to the conclusion that this process is not at all operative in HgTe. The oscillator strength for the Ω_2 phonon [cf. Eq. (8) of Ref. 8] is proportional to

$$P_2 \sim \left| \frac{\langle f|H_2|s\rangle\langle s|H_0|i\rangle}{E_i - E_s - i\gamma(E_s)} \right|^2 \delta(E_i - E_f) , \tag{9}$$

where $|i\rangle$ is the state having a photon with energy $\hbar\omega$ and a TA phonon, $|s\rangle$ is the state having a phonon with energy $\hbar\omega_{\mathrm{TA}}$ and an electron-hole pair with energy E_s, $|f\rangle$ is the final state with a TO($\mathbf{q}$) phonon, H_0 is the Hamiltonian describing electron-photon interaction, and H_2 is the Hamiltonian describing the electron–two-phonon interaction.

The total contribution to the oscillator strength of the TO phonon can be written as

$$P_1 = P_1(\mathrm{ion}) + P_1(\mathrm{electronic}) ,$$

where P_1(ion) is the result of direct photon-lattice interaction and P_1(electronic) is the resonant contribution that can be important where electronic interband transitions are close to the phonon energy. Writing P_1(electronic) explicitly, we have

$$P_1(\mathrm{electronic}) \sim \left| \frac{\langle f'|H_1|s_0\rangle\langle 0|H_0|i_0\rangle}{E_{i_0} - E_{s_0} - i\gamma(E_{s_0})} \right|^2 \times \delta(E_{i_0} - E_{f'}) , \tag{10}$$

where $|i_0\rangle$ is the state having a photon with energy $\hbar\omega$, $|s_0\rangle$ is the state having an electron-hole pair with energy E_{s_0}, $|f'\rangle$ is the final state with a TO($\mathbf{q}=\mathbf{0}$) phonon, and H_1 is the Hamiltonian describing the electron–one-phonon interaction.

It can be argued that P_1(electronic) should show a strong temperature dependence[8] whereas P_1(ion) is temperature "independent." Grynberg *et al.*[2] find P_1 as independent of temperature. Thus one can conclude that P_1(electronic) *is negligibly small.* Also, since the photon energies involved are similar (~ 100 cm^{-1} for Ω_2 and 118 cm^{-1} for the TO phonon), the matrix elements $\langle s|H_0|i\rangle$ [Eq. (9)] and $\langle s_0|H_0|i_0\rangle$ [Eq. (10)] should be nearly equal. Dividing (9) by (10), we have

$$\frac{P_2}{P_1(\mathrm{electronic})} = \left| \frac{\langle f|H_2|s\rangle}{\langle f'|H_1|s_0\rangle} \right|^2 . \tag{11}$$

Though symmetry considerations do not rule out a nonzero value for $\langle f|H_2|s\rangle$,[8] it can be argued that the value of this matrix element should be vanishingly small. This matrix element involves simultaneous destruction of a large-$|\mathbf{q}|$ acoustic phonon and creation of a large-$|\mathbf{q}|$ optic phonon [see Fig. 4(a)]. Therefore, its explicit evaluation would involve the electron-phonon interaction to second order in perturbation theory. Neglecting the TA-phonon energy (~ 20 cm^{-1}) the denominator would involve the difference in energy of electron (hole) states at $\mathbf{k}$ and $\mathbf{k}+\mathbf{q}$. Thus for a significant value of $\langle f|H_2|s\rangle$, the energies of state $\mathbf{k}$ and $\mathbf{k}+\mathbf{q}$ should be nearly the same. This sort of situation is encountered in materials having a partially occupied *d* band such as TiN, ZrN, NbC, TaC, etc.[18] The *d* band, being flat in energy, has similar energies for states differing by a large $\mathbf{q}$. In materials without *d* bands or completely filled (empty) *d* bands, the two-phonon spectra are extremely weak or not seen at all.[18] In HgTe, there are no partially occupied flat bands. Here, both the conduction and the valence bands have strong dispersion (for a description of band structure, see Ref. 1) and for the $\mathbf{q}$ involved the energy difference would be very large (~ 1 eV) for all $\mathbf{k}$'s of interest. Thus one expects the ratio defined in Eq. (11) to be very small, leading to a still smaller value for the ratio P_2/P_1 contrary to experimentally observed large P_2.

Moreover, the "resonance enhancement" argument advanced by the authors of Ref. 8 is not valid for $Hg_{1-x}Cd_xTe$. Baars and Sorger[3] observe this additional feature Ω_2 up to $x = 0.34$. Using[19]

$$E_G = -300 + 0.5T + (1910 - T)x \text{ meV} ,$$

where T is the temperature in degrees Kelvin. With

$T=77$ K,[3] the gap turns out to be ~ 360 mV for $x=0.34$. Thus there are no interband electronic transitions matching the difference phonon energy. The observation thus rules out the "two-phonon resonance enhancement" as the cause of large oscillator strength for the Ω_2 mode.

It follows from the mode-coupling theory given here that if Ω_D moves significantly away from ω_{TO}, then Ω_2 shall have vanishing intensity. In CdTe ($x=1$), for which information about the density of states is available,[10] $(\omega_{TO}-\Omega_D)$ is indeed large (~ 35 cm^{-1}) and the Ω_2 mode is not seen experimentally. We therefore believe that it is this change of dispersion curves with increasing x that makes Ω_D move away from ω_{TO}, resulting in a negligibly small intensity for the Ω_2 mode.

A crude estimate can be made of the expected oscillator strength associated with the Ω_2 mode in HgTe on the basis of a Fermi resonance. In Eq. (1) the thermal factor $[n(\omega)+1]$ can be deleted and the line shape again calculated, which is merely $\chi''(\omega)$. The two peaks in the resulting line shape can be fitted with two Lorentzians. Using

$$P_2' = \int_{\text{band}} \frac{\epsilon''(\omega)}{\omega} d\omega ,$$

the oscillator strength associated with the Ω_2 oscillator relative to the TO-phonon-mode strength can be estimated. We get a value of 1.8 for the Ω_2 mode (TO-phonon mode $P_1 \sim 4.7$) at room temperature, which compares very well with the value of 2.5 deduced from ir experiments.[2]

V. CONCLUSIONS

We have shown that in HgTe, the additional mode which appears in ir and Raman spectra below the TO-phonon frequency is a combination mode that derives its intensity from the TO-phonon mode. Using the mode-coupling formulation, we have explained the observed frequency shift and spectral intensity variation with the temperature. It also provides a natural explanation for the occurrence of this feature in Hg-rich $Hg_{1-x}Cd_xTe$ alloys.

ACKNOWLEDGMENTS

We gratefully acknowledge Dr. A. V. R. Warrier (Solid State Physics Laboratory, New Delhi) and Professor A. K. Ramdas (Purdue University) for providing HgTe single crystals. We are thankful to Dr. B. A. Dassanacharya for his keen interest in this work.

*Present address: Non-Linear Optics Group, Laser Programme, Centre for Advance Technology, Indore 452 012, India.

[1] R. Dornhaus and G. Nimtz, in *Narrow Gap Semiconductors,* edited by G. Höhler, Springer Tracts in Modern Physics Vol. 98 (Springer, Berlin, 1983).

[2] M. Grynberg, R. LeToullec, and M. Balkanski, Phys. Rev. B **9**, 517 (1974).

[3] J. Baars and F. Sorger, Solid State Commun. **10**, 875 (1972).

[4] S. W. McKnight, P. M. Amirtaraj, and S. Perkowitz, Solid State Commun. **25**, 357 (1978).

[5] Alka Ingale, M. L. Bansal, and A. P. Roy, Phys. Rev. B **40**, 12 353 (1989).

[6] H. Kepa, W. Gebicki, T. Giebultowicz, B. Buras, and K. Glausen, Solid State Commun. **34**, 211 (1980).

[7] P. Swiatek, A. M. Witowski, and M. Grynberg, Phys. Status Solidi B **89**, K1 (1978).

[8] A. M. Witowski and M. Grynberg, Phys. Status Solidi B **100**, 389 (1980).

[9] A. M. Witowski and M. Grynberg, Solid State Commun. **30**, 4 (1979).

[10] D. N. Talwar and M. Vandevyver, J. Appl. Phys. **56**, 1601 (1984).

[11] Alka Ingale, Ph.D. thesis, Bombay University, 1989.

[12] J. F. Scott, *Light Scattering in Solids,* edited by M. Balkanski (Flammarion, Paris, 1968), p. 387.

[13] R. S. Katiyar, J. F. Ryan, and J. R. Scott, Phys. Rev. B **4**, 2635 (1971).

[14] A. S. Barker, Jr. and J. J. Hopfield, Phys. Rev. **135**, A1732 (1964).

[15] J. F. Scott, Rev. Mod. Phys. **46**, 83 (1974).

[16] J. F. Scott, Phys. Rev. Lett. **21**, 907 (1968).

[17] R. Trommer. H. Muller, M. Cardona, and P. Vogl, Phys. Rev. B **21**, 4869 (1980).

[18] M. V. Klein, in *Light Scattering in Solids III,* edited by M. Carbona and G. Güntherodt, Topics in Applied Physics Vol. 51 (Springer-Verlag, Berlin, 1982).

[19] J. D. Wiley and R. N. Dexter, Phys. Rev. **181**, 1181 (1961).